Supporting Information

Promotion or suppression of hydrogen evolution activity? The competition between sodium cations and quaternary ammonium ions at the metal/water interface

Shilin Bo,[a] Yang Xiang,[a] Qiong Xiang,[a] Li Li,[a] Xun Huang[a], Zidong Wei *[a]*

[a] Center of Advanced Electrochemical Energy, State Key Laboratory of Advanced Chemical Power Sources, School of Chemistry and Chemical Engineering, Chongqing University, Chongqing 40004 (P. R. China); E-mail: huangxun@cqu.edu.cn; zdwei@cqu.edu.cn

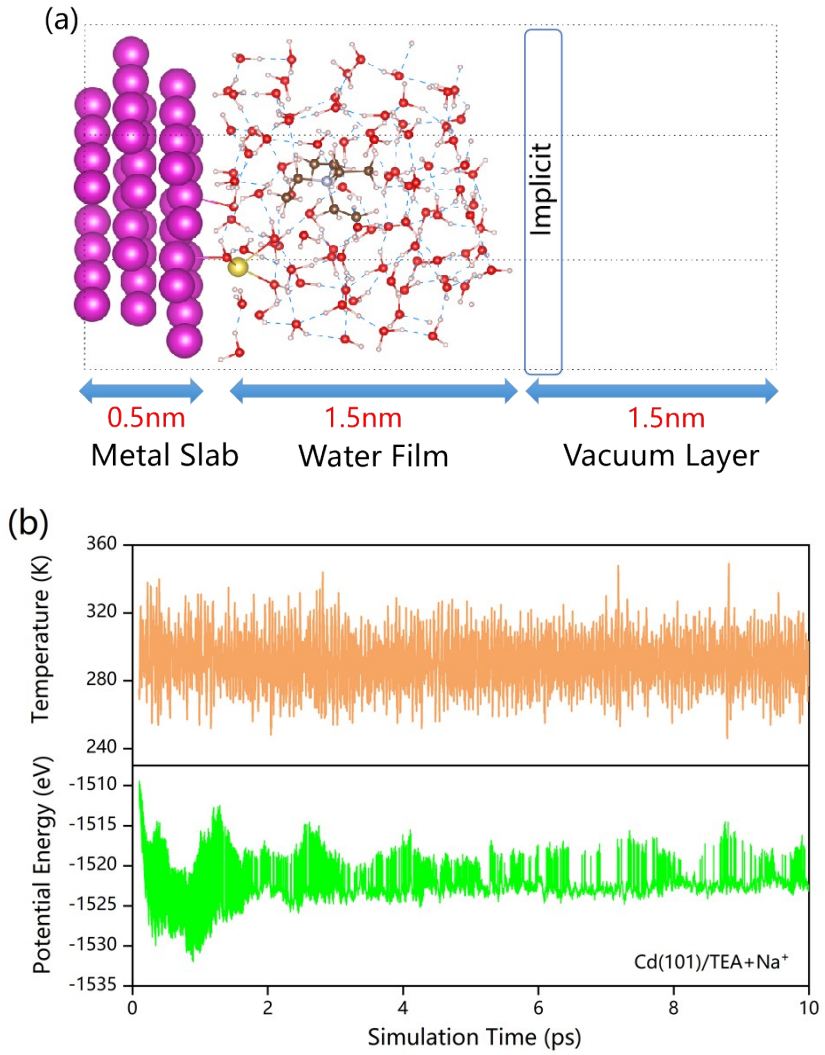

Figure S1 (a) The schematic of metal/water interface model. (b) Variation of temperature and energy with simulation time in Cd(101)/water(TEA) interface.

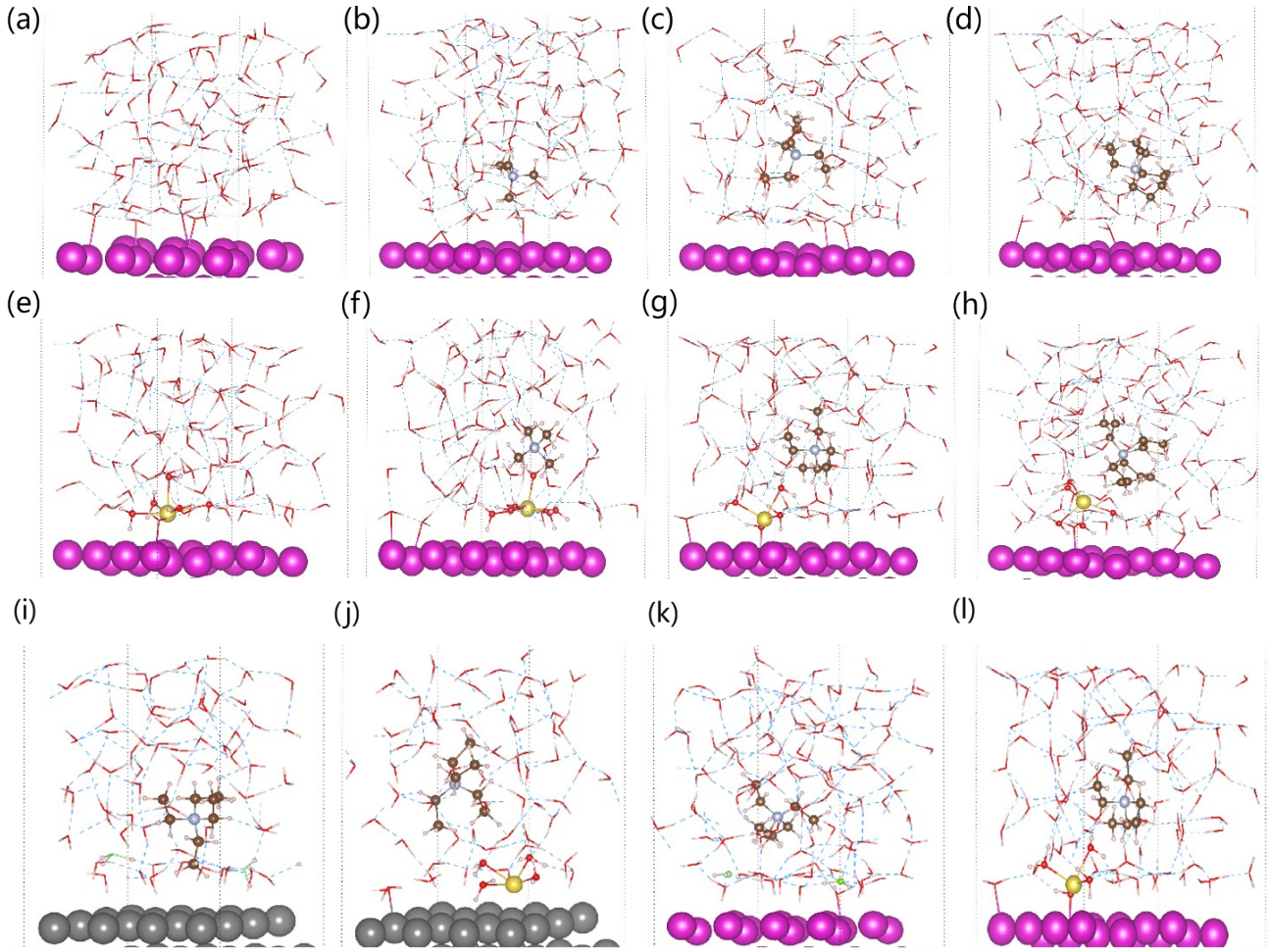

Figure S2 Snapshots of AIMD simulations. (a~d) H_2O, TMA, TEA and TPA in Cd(101), (e~h) H_2O, TMA, TEA and TPA in Cd(101) with Na^+, (i) Pt(111)/TEA under acidic condition, (j) Pt(111)/TEA under alkaline condition, (k) Cd(101)/TEA acidic condition, (l) Cd(101)/TEA under alkaline condition.

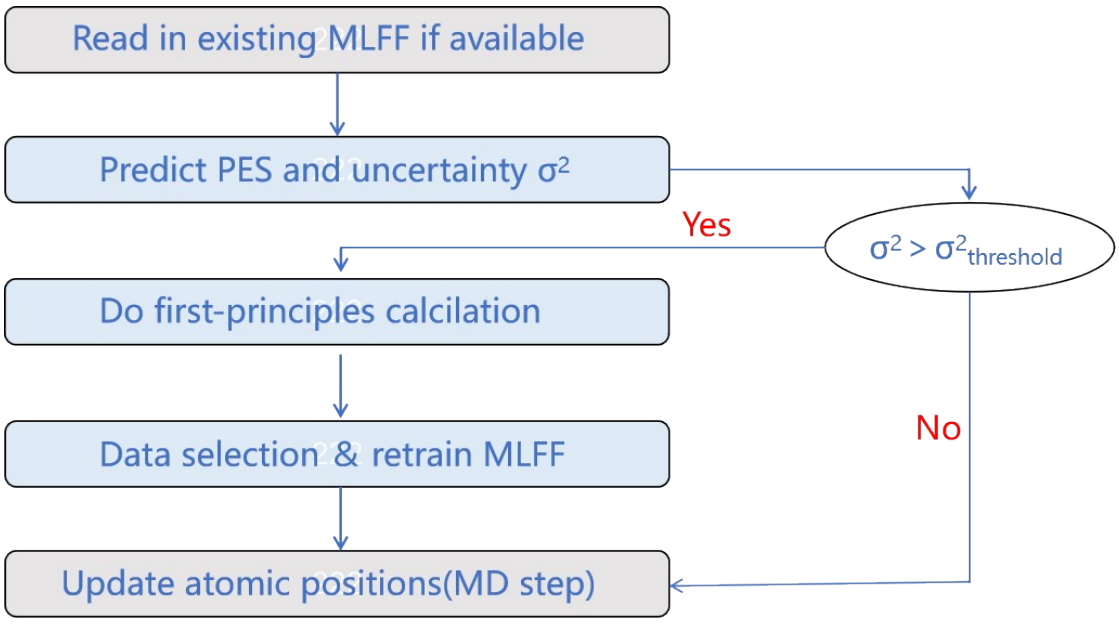

Figure S3 On-the-fly machine learning force field generation using Bayesian linear regression (ML-AIMD)

During the molecular dynamic simulation process, a machine learning potential is automatically generated within VASP software, with first-principles calculations being performed only when new configurations exceed the already sampled dataset as shown in Figure S3, this method has been applied to calculate the molecular dynamics simulation of the electrocatalytic solid-liquid interface double layer. The application results indicate that over 50% of first-principles calculations were bypassed during the force field generation process.[1] This allows the machine to rapidly construct a first-principles dataset across a wide phase space. Moreover, with the aid of the generated machine learning potential, the simulation speed was nearly double that of first-principles calculations, with tasks that would typically take traditional AIMD only requiring 5 days using ML-AIMD, While saving on computational cost and time, the accuracy of the calculations is also ensured.[2, 3]

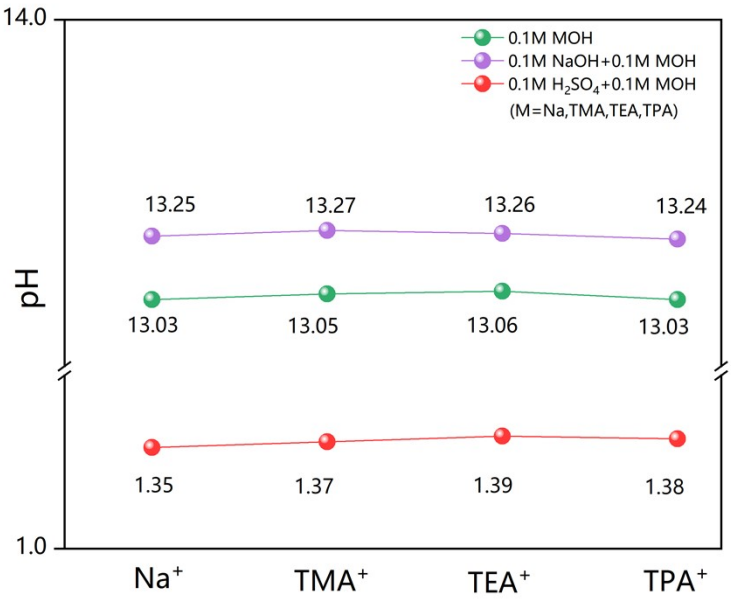

Figure S4 The pH of the electrolytes used for LSV test.

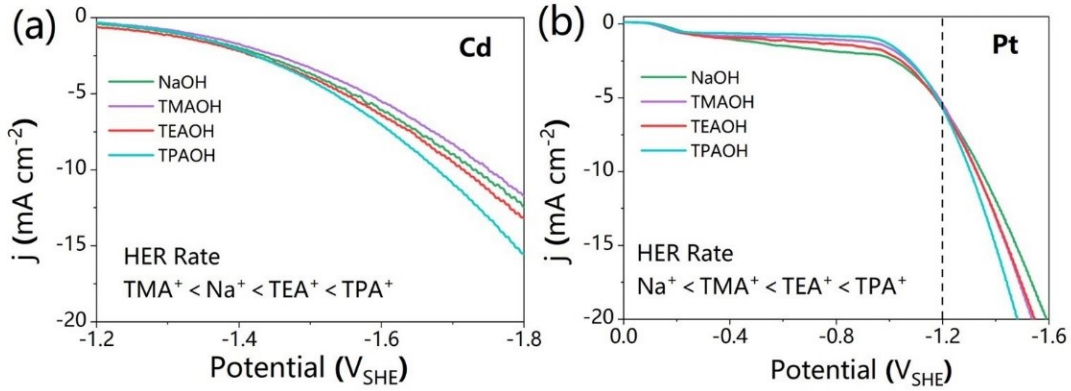

Figure S5 LSV polarization curves on Cd and Pt electrodes in different electrolytes without stirring.

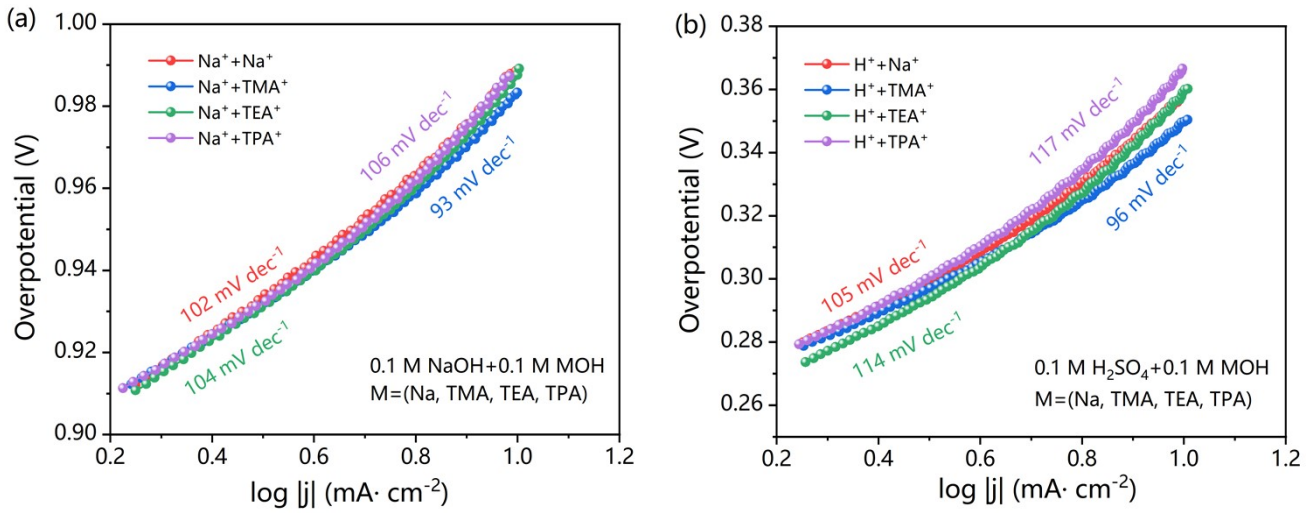

Figure S6 Tafel slopes of different electrolyte molecules for the HER reaction under acidic and alkaline conditions on Pt.

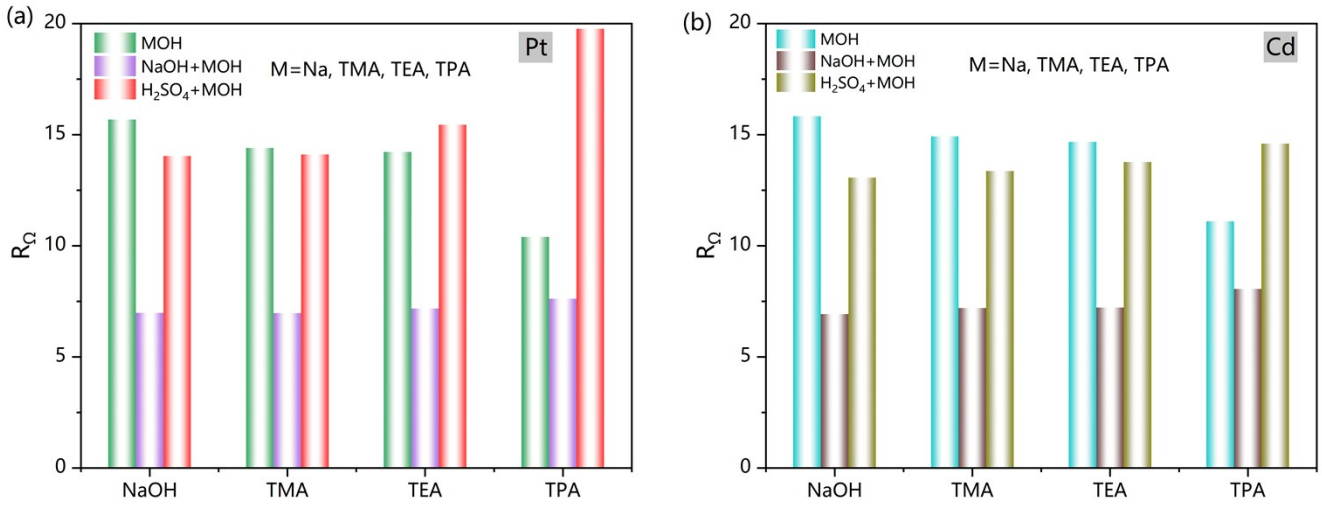

Figure S7 Solution resistances measured of EIS in different electrolytes. (a) Pt electrode; (b) Cd electrode.

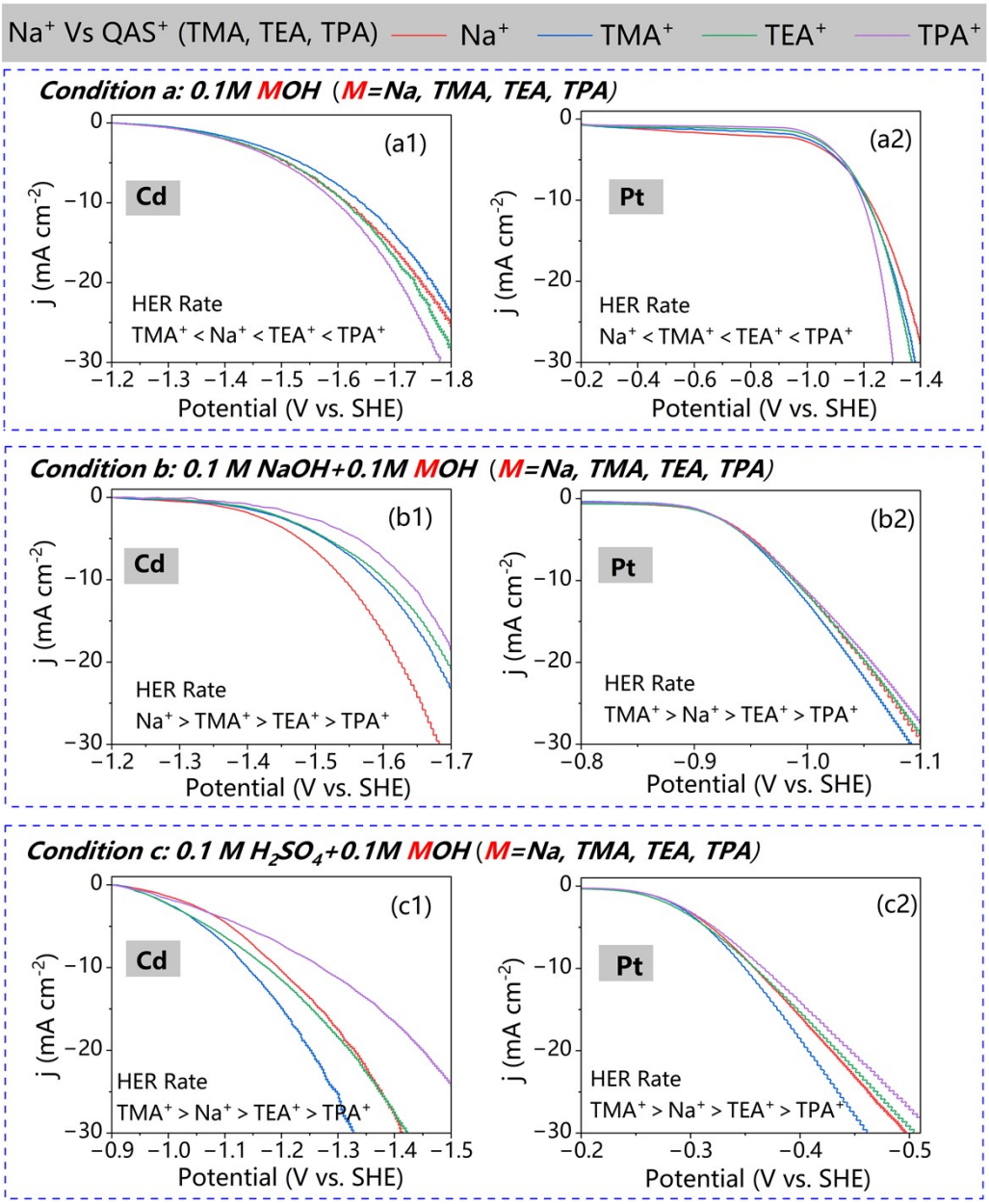

Figure S8 IR compensated LSV curves in different electrolytes.

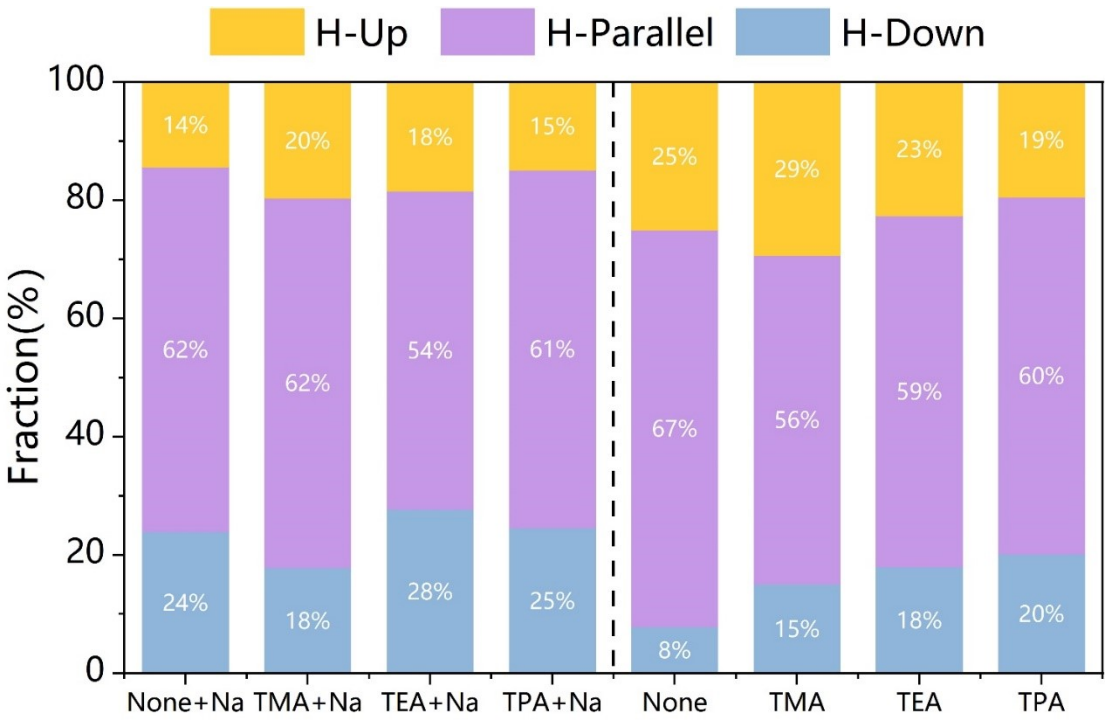

Figure S9 Orientation ratio of water molecules in the electrical double layer.

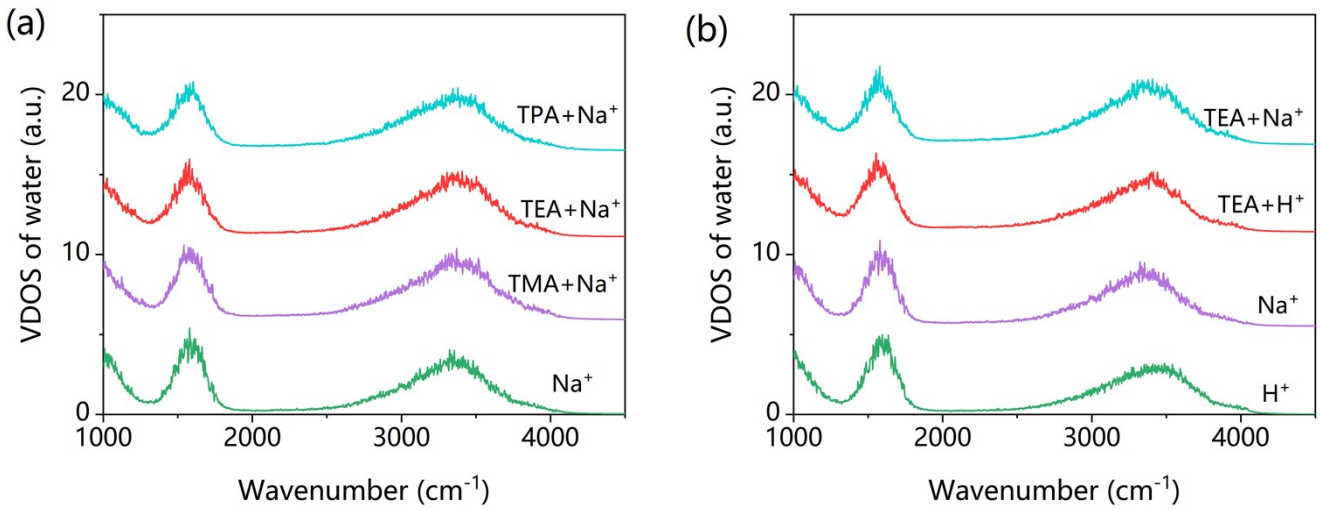

Figure S10 VDOS water molecules at Cd(101)/water interfaces with different cations. (a) Effect of QAS in the presence of Na^+; (b) Comparison of Na^+ and H^+ with or without TEA.

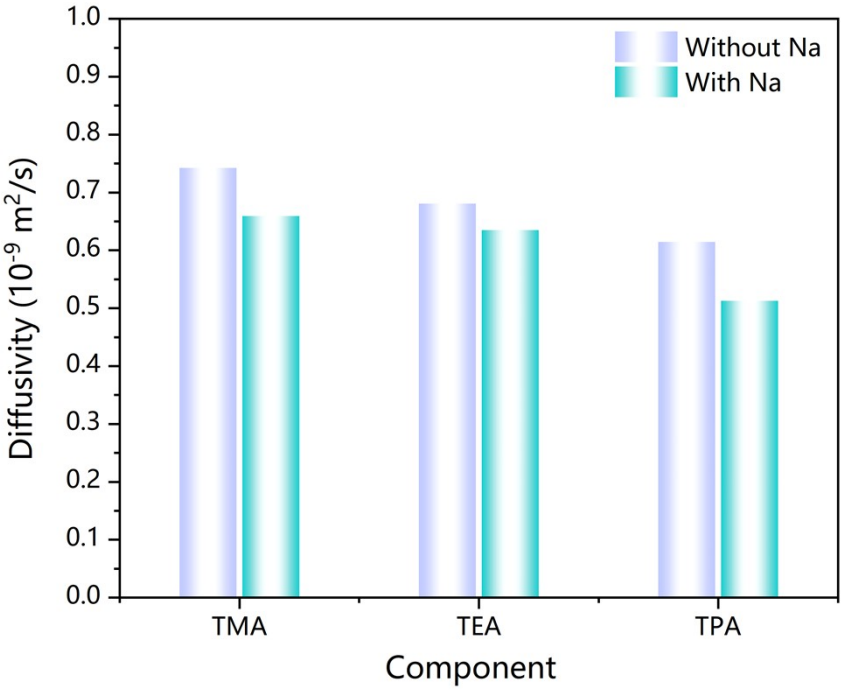

Figure S11 Diffusion coefficients of QAS with and without the presence of Na^+.

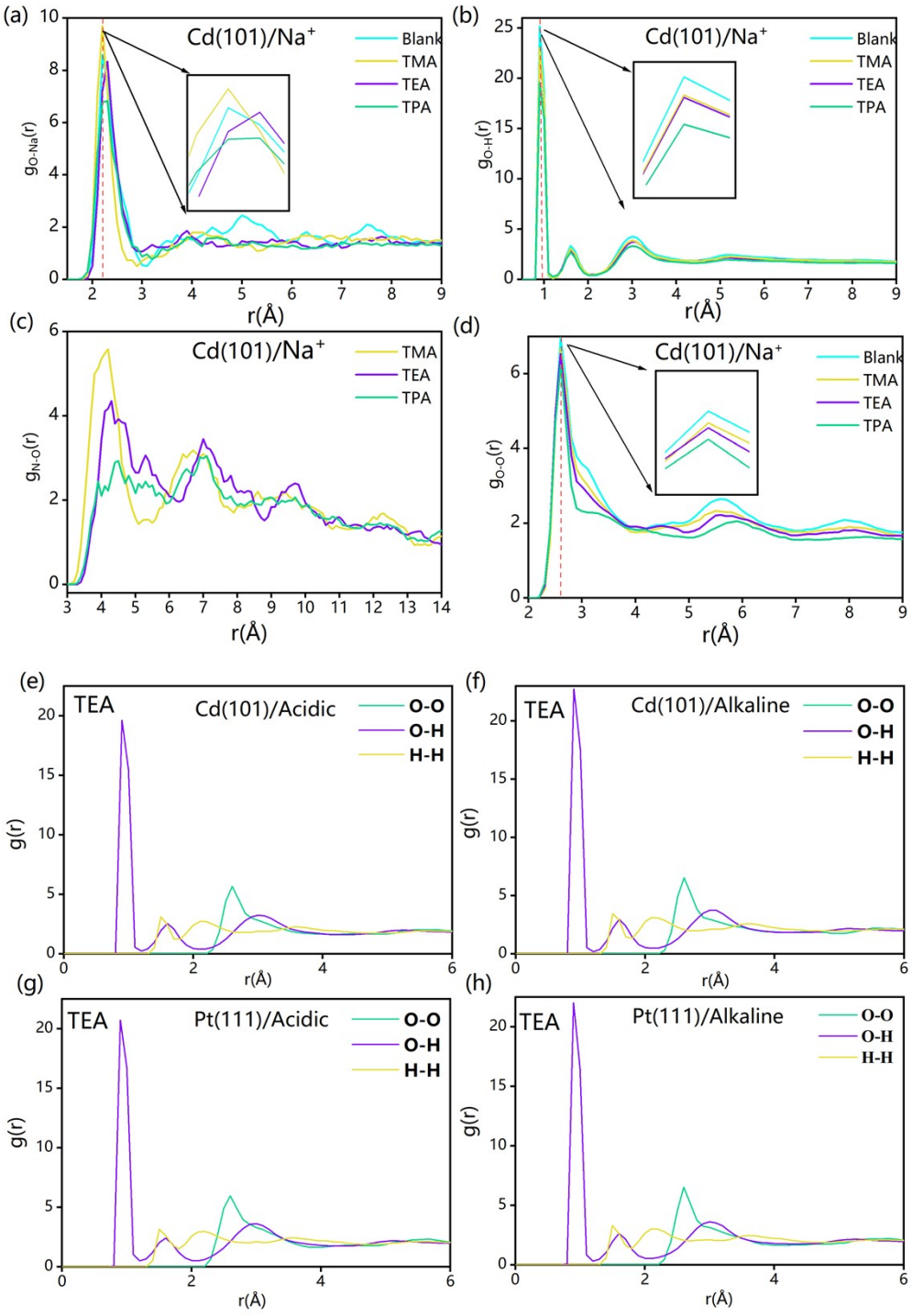

Figure S12 (a~d) RDF of QAS of different chain lengths to Cd (101) under alkaline conditions. (e~f) are the radial distribution functions $g_{O\text{-}H}(r)$, $g_{O\text{-}O}(r)$, and $g_{H\text{-}H}(r)$ for a Cd electrode in acidic and alkaline environments, (g~h)are the radial distribution functions $g_{O\text{-}H}(r)$, $g_{O\text{-}O}(r)$,and $g_{H\text{-}H}(r)$ for a Pt electrode in acidic and alkaline environments.

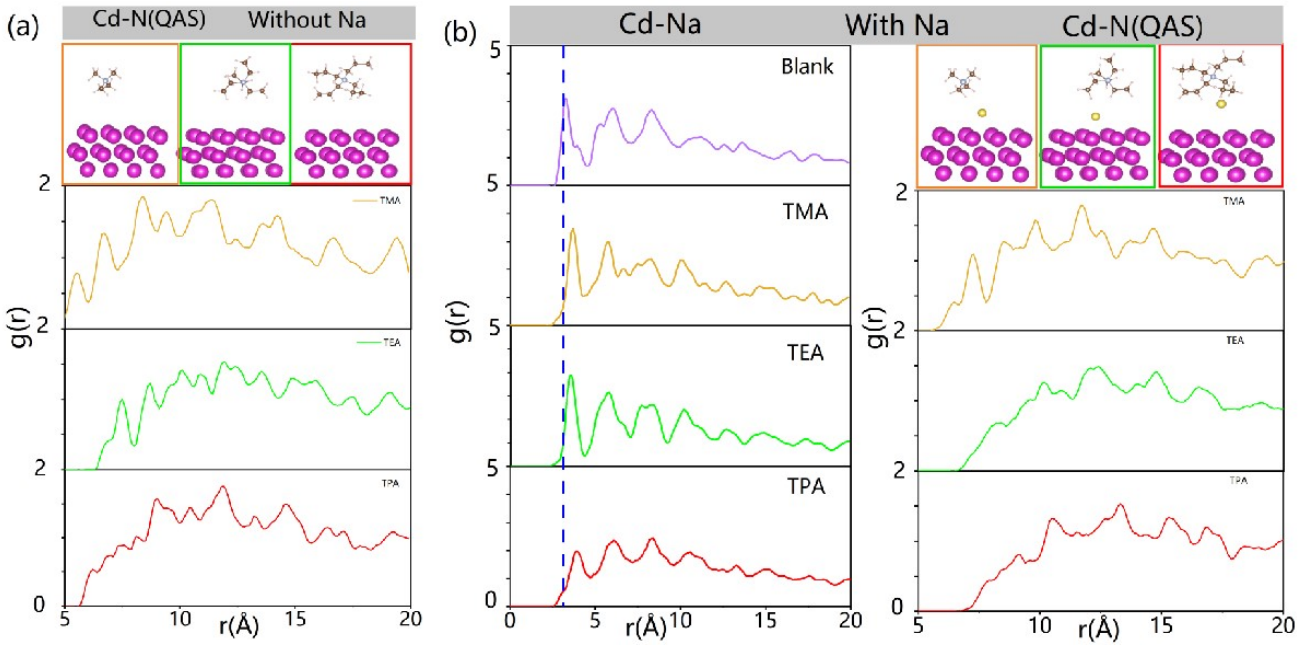

Figure S13 (a) RDF of Cd-N in electrolytes without Na; (b) RDF of Cd-Na and Cd-N in electrolyte with Na.

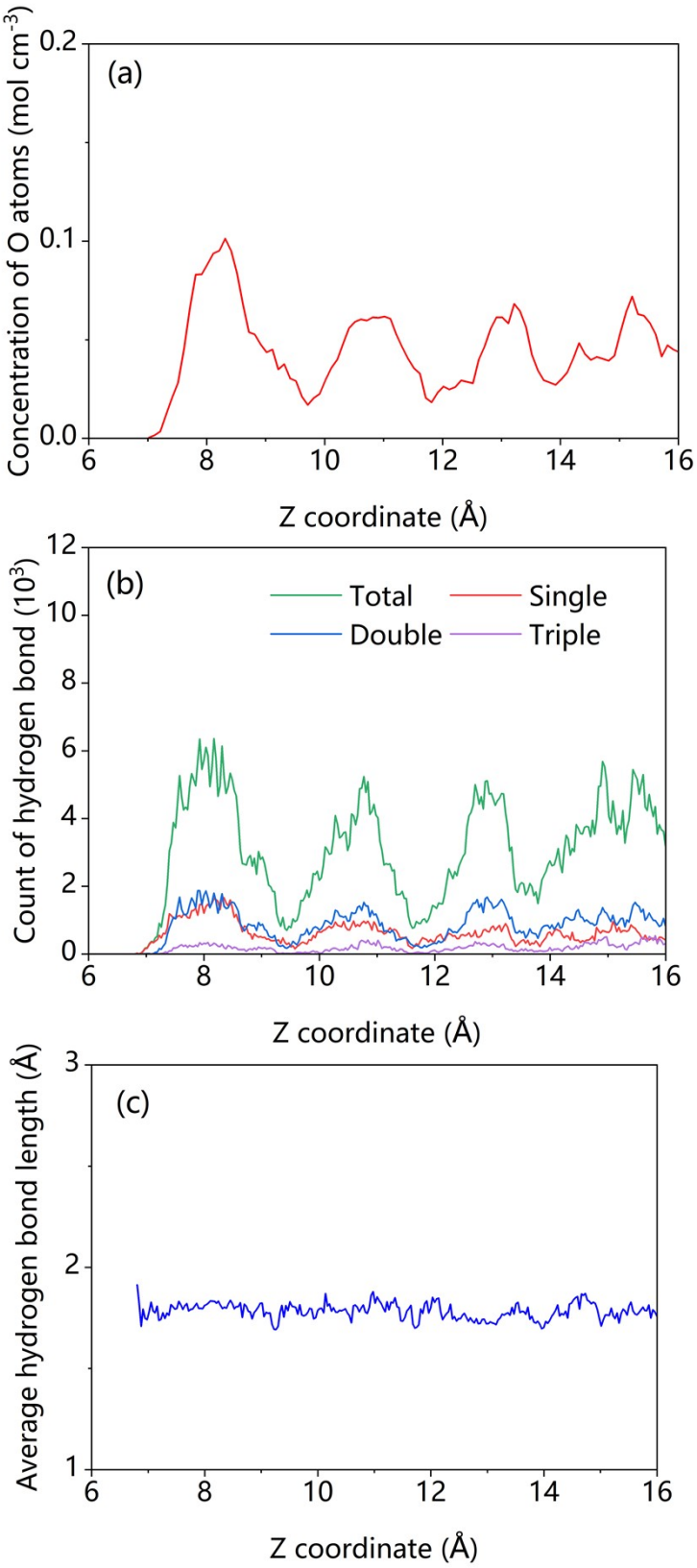

Figure S14 Profiles along Z coordinate of Cd(101)/ /water interface under acid condition. (a) Water distribution; (b) Hydrogen bond number; (c) Average hydrogen bond length.

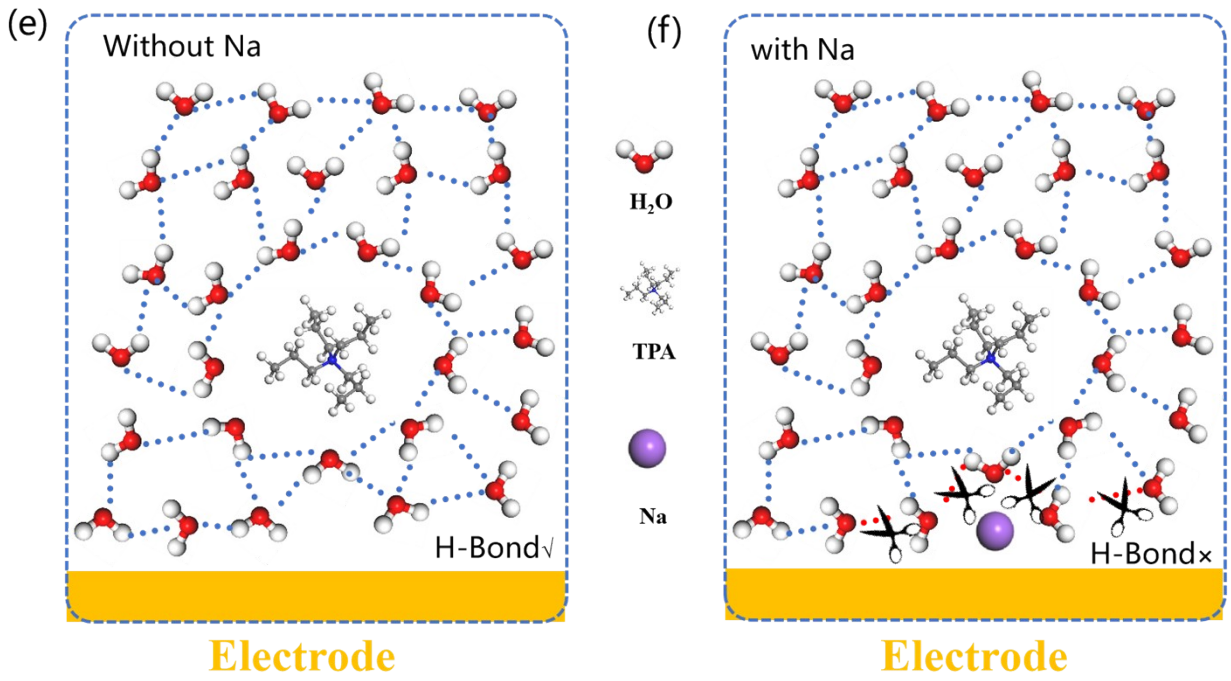

Figure S15 Scheme of hydrogen bond network structure (e)with and (f)without Na^+

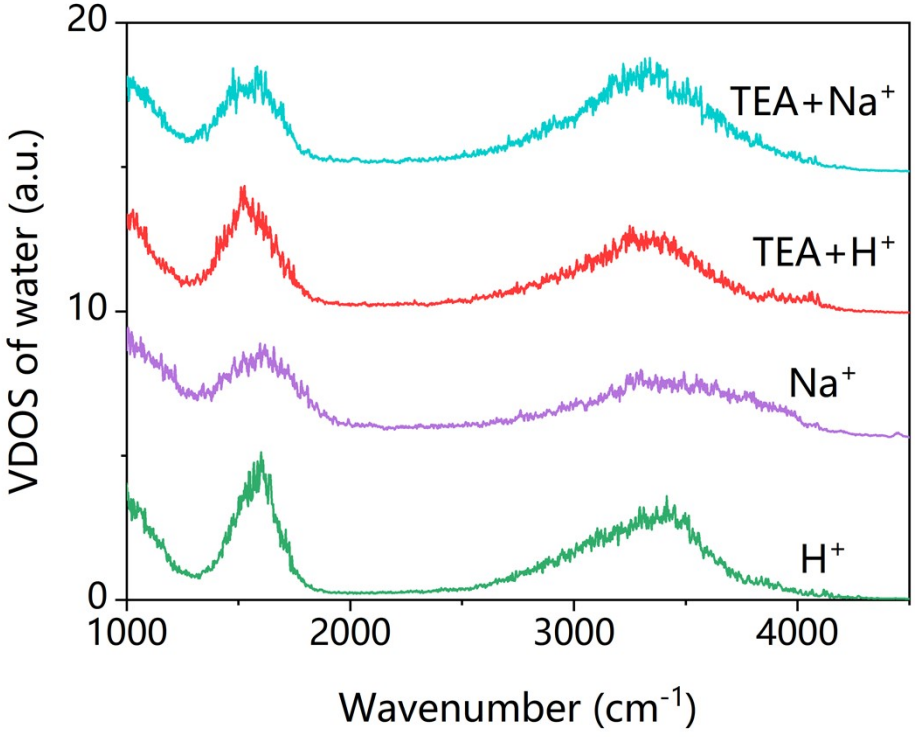

Figure S16 Comparison of Na^+ and H^+ with or without TEA at Pt(101)/water interfaces.

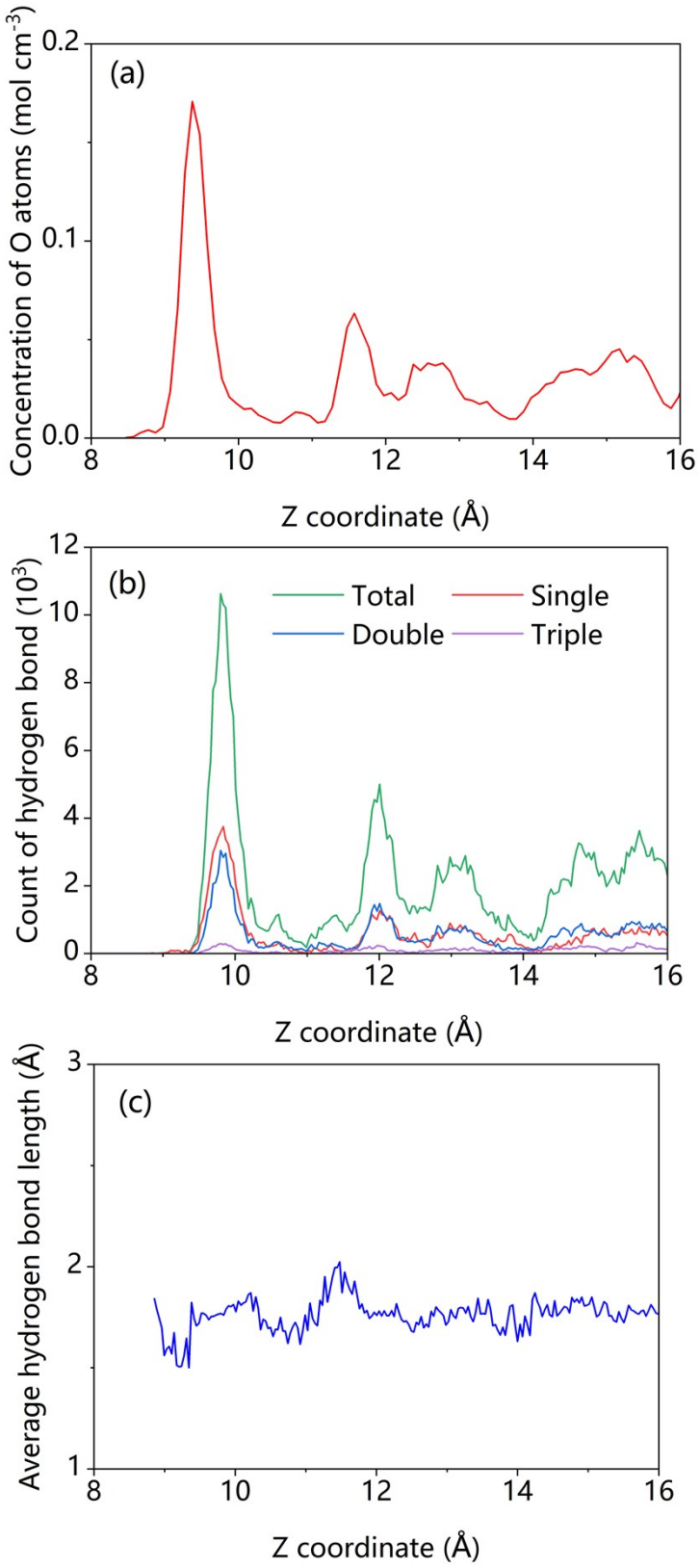

Figure S17 Profiles along Z coordinate of Pt(111)/water interface under Acid condition. (a) Water distribution; (b) Hydrogen bond number; (c) Average hydrogen bond length.

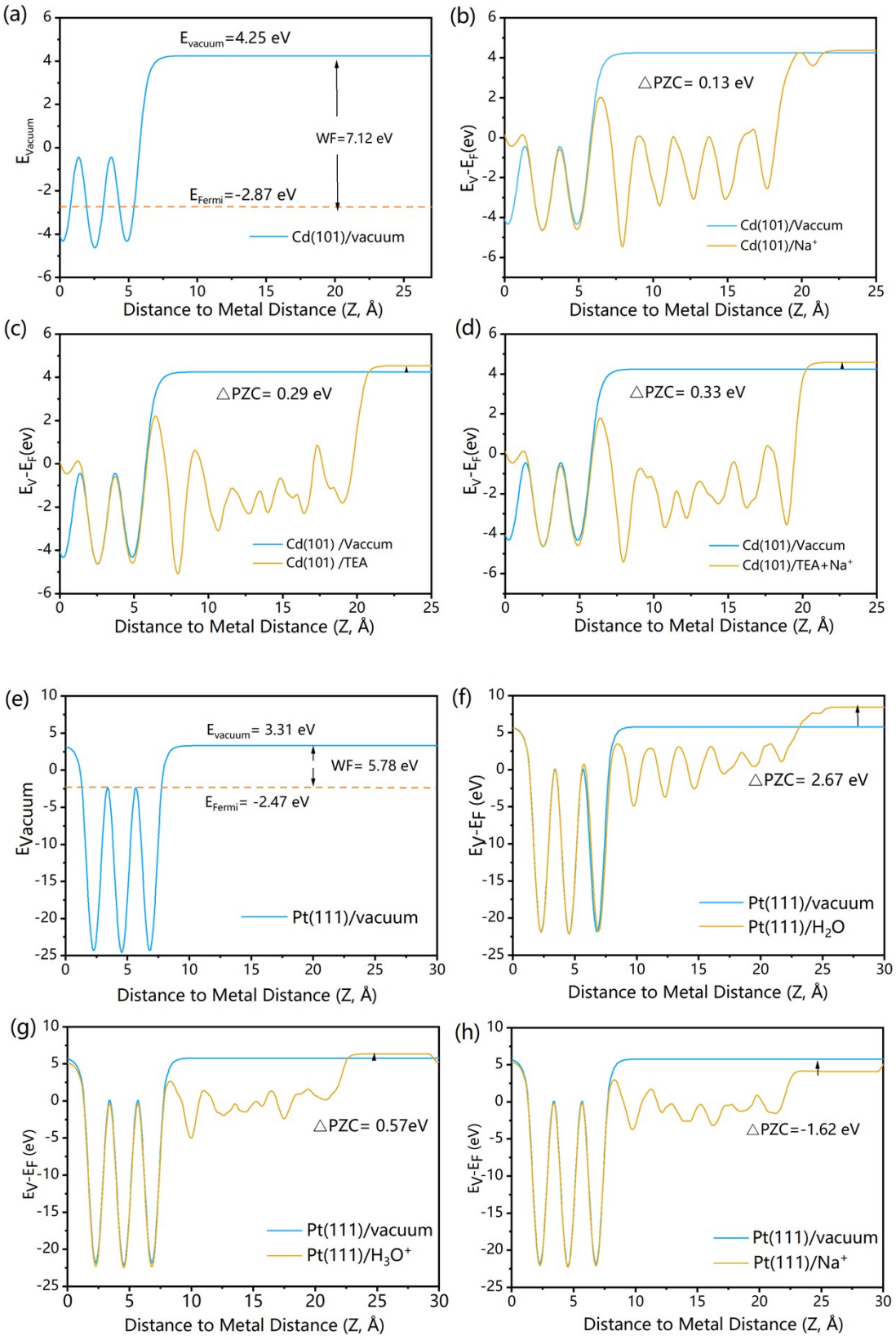

Figure S18 Electrostatic potential distribution of Cd(101) and Pt(111) interface.

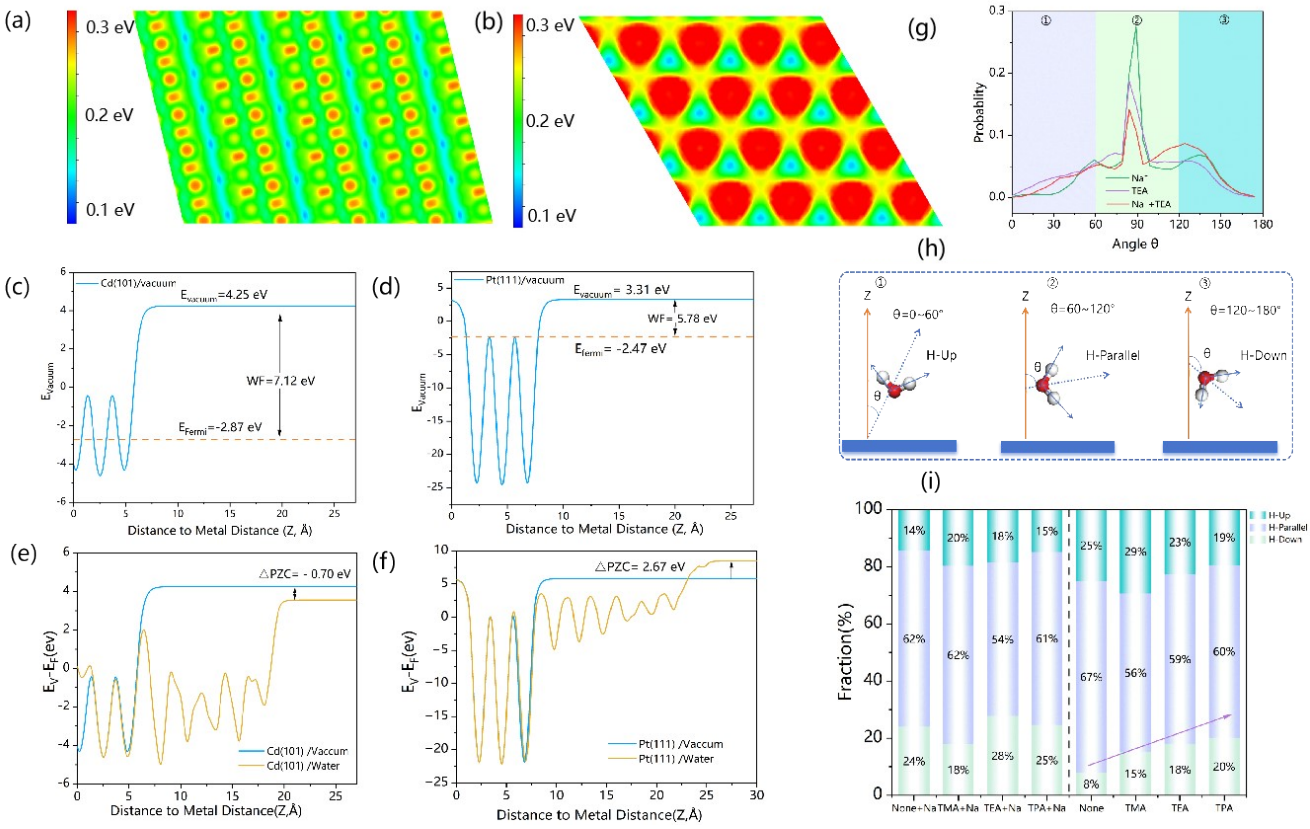

Figure S19 Comparison of electronic properties of Cd and Pt. (a) Electronic local density function at Cd(101) surfaces, (b) Electronic local density function at Pt(111) surfaces;,(c)Work function of Cd(101) vacuum, (d) Work function of Pt(111) vacuum, (e) Work function of Cd(101)/water, (f) Work function of Pt(111)/water, (g) Statistical orientation distribution of water molecules with Na^+, TEA and Na^++TEA, (h) Schematic diagram of water molecules in different orientations, (i) Schematic diagram of the statistical proportions of water molecules in different orientations.

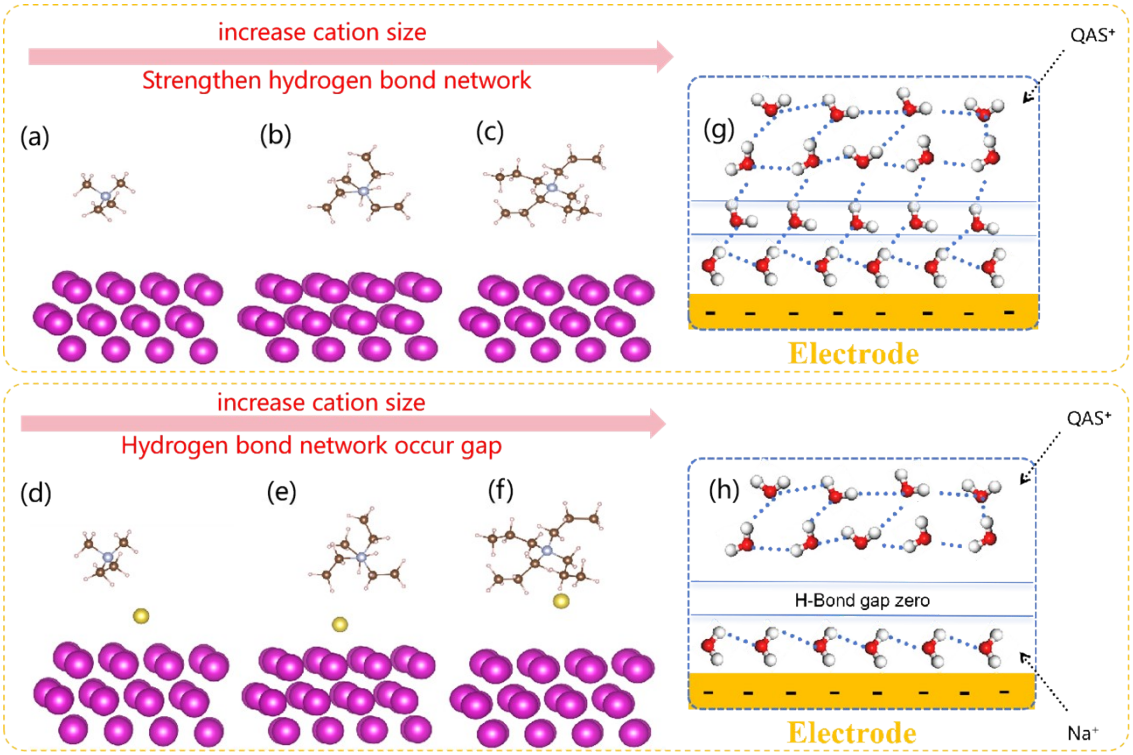

Figure S20 (a-c) Local schematic diagram of the QAS Cd(101) interface model. (d-f) Local schematic diagram of the Cd (101) interface model with the synergistic effect of QAS and Na^+. (g) A schematic diagram showing how the addition of QAS enhances the hydrogen bond network. (h) A schematic diagram illustrating the layered structure of the hydrogen bond network resulting from the synergistic effect of QAS and Na^+.

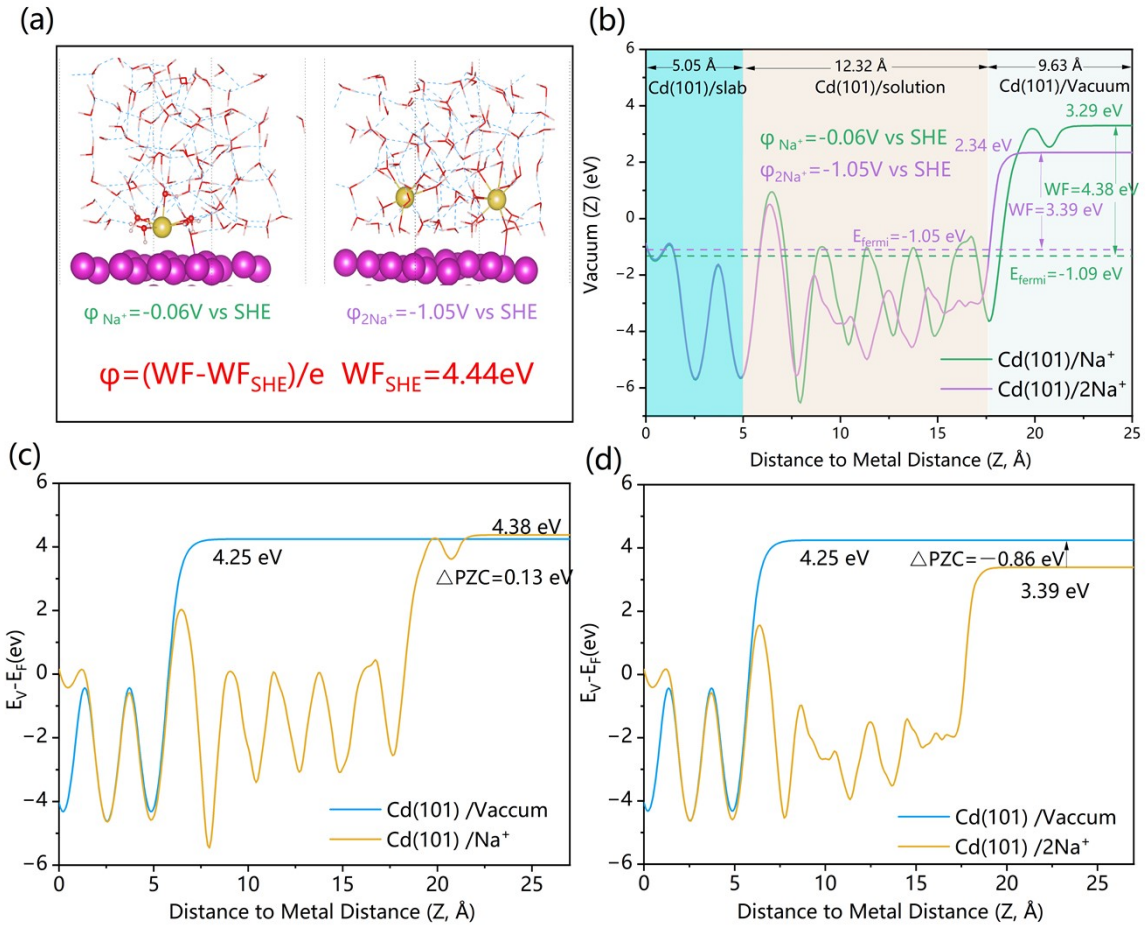

Figure S21 (a) Schematic diagram of the interface structure of Na and 2Na, (b) Calculation method for electrode potential, (c) Interface electrode potential of Na, (d) Interface electrode potential of 2Na

---

The PZC can be obtained by the following equation.

$$\phi_{Na^+} = \frac{WF - WF_{SHE}}{e} = \frac{4.38\ eV - 4.44\ eV}{e} = -0.06\ V$$

$$WF - WF_{SHE} = 3.39\ eV - 4.44\ eV$$

Where WF_{SHE} is the thermodynamic work function of the standard hydrogen electrode (SHE). Using the value of 4.44 eV suggested by Trasatti[4], which has also been widely applied in many electrochemical and surface science studies[4-6].

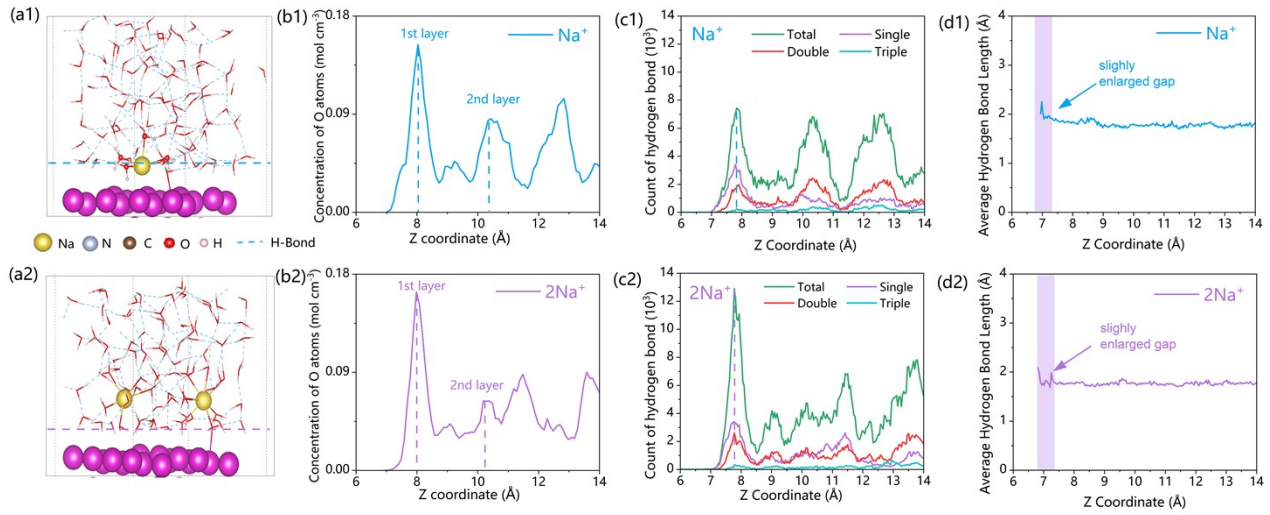

Figure S22 (a1 a2) Snapshots of AIMD simulations in Cd(101)/Na^+ and Cd(101)/$2Na^+$ (b1 b2) Oxygen atom density profile along the z-axis with different cations present in Cd(101)/Na^+ and Cd(101)/$2Na^+$, (c1 c2) Statistical analysis of single, double, and triple hydrogen bonds with different cations in Cd(101)/Na^+ and Cd(101)/$2Na^+$, (d1 d2) Statistical analysis of average hydrogen bond lengths along the Z-axis of the Cd (101) crystal plane in Cd(101)/Na^+ and Cd(101)/$2Na^+$.

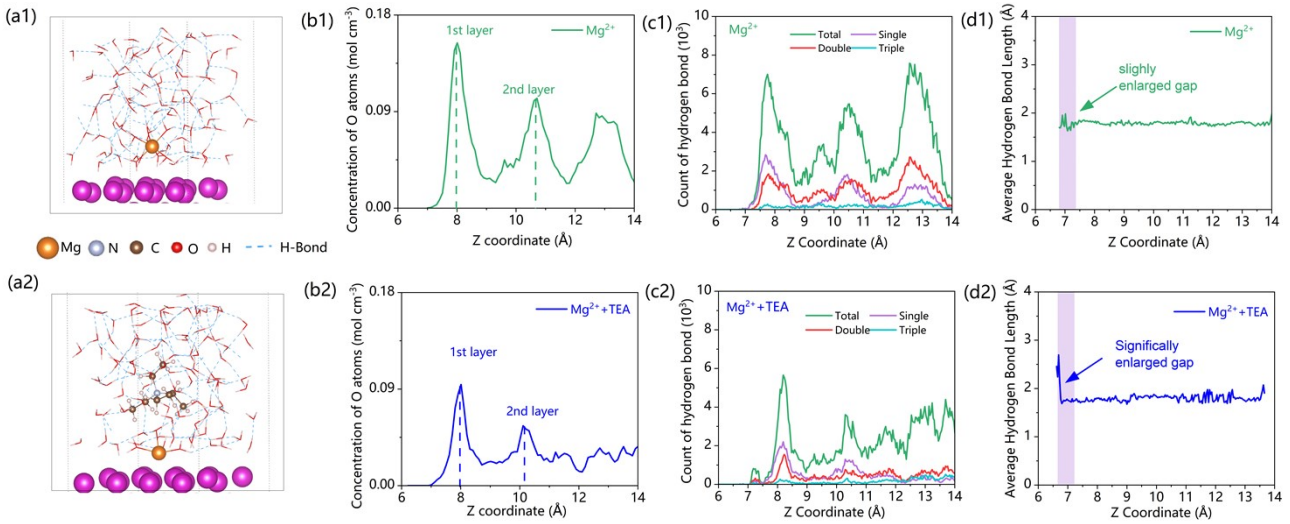

Figure S23 (a1 a2) Snapshots of AIMD simulations in Cd(101)/Mg^{2+} and Cd(101)/ Mg^{2+}+TEA, (b1 b2) Oxygen atom density profile along the z-axis with different cations present in Cd(101)/Mg^{2+} and Cd(101)/ Mg^{2+}+TEA, (c1 c2) Statistical analysis of single, double, and triple hydrogen bonds with different cations in Cd(101)/Mg^{2+} and Cd(101)/ Mg^{2+}+TEA, (d1 d2) Statistical analysis of average hydrogen bond lengths along the Z-axis of the Cd (101) crystal plane in Cd(101)/Mg^{2+} and Cd(101)/ Mg^{2+}+TEA.

Table S1 List of Experimental Reagents and Materials

Types of drugs	Standard	Manufacturer
H_2SO_4	98%	Chongqing ChuanDong Chemical (Group) Co., Ltd.
NaOH	98%	Shanghai Aladdin Biochemical Technology Co., Ltd.
MgOH	98%	Shanghai Aladdin Biochemical Technology Co., Ltd.
TMAOH	75 wt%	Shanghai Mireille.
TEAOH	75 wt%	Shanghai Mireille.
TPAOH	75 wt%	Shanghai Mireille.
Cd	99.9%	Shanghai Chaowei Nano Technology Co., Ltd.
Pt	99.9%	Shanghai Chaowei Nano Technology Co., Ltd.

e

Table S2 List of Calculation model with EDL

Types of Model	Theory	Calculation type
Cd (101)	Interface environment theory.	DFT
Pt (111)	Interface environment theory.	DFT
Cd (101)/H_2O	Interface environment theory.	DFT
Pt (111)/H_2O	Interface environment theory.	DFT
Cd (101)/H_2O	Interface environment theory.	AIMD (10ps)
Cd (101)/TMA	Interface environment theory.	AIMD (10ps)
Cd (101)/TEA	Interface environment theory.	AIMD (10ps)
Cd (101)/TPA	Interface environment theory.	AIMD (10ps)
Cd (101)/Na^++TMA	Interface environment theory.	AIMD (10ps)
Cd (101)/Na^++TEA	Interface environment theory.	AIMD (10ps)
Cd (101)/Na^++TPA	Interface environment theory.	AIMD (10ps)
Cd (101)/H_3O^++TEA	Interface environment theory.	AIMD (10ps)
Pt (111)/ H_3O^+	Interface environment theory.	AIMD (10ps)
Pt (111)/ H_2O	Interface environment theory.	AIMD (10ps)
Pt (111)/Na^++TEA	Interface environment theory.	AIMD (10ps)
Pt (111)/ H_3O^++TEA	Interface environment theory.	AIMD (10ps)
Pt (111)/Cs^+	Interface environment theory.	AIMD (10ps)
Pt (111)/Cs^++TEA	Interface environment theory.	AIMD (10ps)

Reference

1 R. Jinnouchi, F. Karsai, G. Kresse, Physical Review B 2019, 100, 014105.

2 O. T. Unke, S. Chmiela, H. E. Sauceda, M. Gastegger, I. Poltavsky, K. T. Schutt, A. Tkatchenko, K.-R. Müller, Chemical Reviews 2021, 121, 10142-10186.

3 V. Botu, R. Batra, J. Chapman, R. Ramprasad, The Journal of Physical Chemistry C 2017, 121, 511-522.

4 S. Trasatti, Pure and Applied Chemistry 1986, 58, 955-966.

5 J. Le, M. Iannuzzi, A. Cuesta, J. Cheng, Physical review letters 2017, 119, 016801.

6 T. Cheng, L. Wang, B. V. Merinov, W. A. Goddard III, Journal of the American Chemical Society 2018, 140, 7787-7790.